Thermal Degradation Phenomena of Polymer Film on Magnet Wire for Electromagnetic Coils

Open Access Pre-Print of DOI: 10.1109/TIA.2020.3040201

Thermal Degradation Phenomena of Polymer Film on Magnet Wire for Electromagnetic Coils

Darren F. Kavanagh, *Member, IEEE,* Konstantinos N. Gyftakis, *Senior Member, IEEE,* and Malcolm D. McCulloch *Senior Member, IEEE*

***Abstract*—Polymer film insulation degradation is a major problem for electric machines which leads to short circuits, overheating and eventually the occurrence of catastrophic failure. Electrical insulation materials provide the vital function of turn-to-turn, phase to phase, and phase-to-ground electrical isolation for the electromagnetic coils and windings. This paper investigates the characterisation of early-onset degradation of thin-film magnet wire insulation at elevated temperatures from 200 to 275 °C. Sample specimens were analysed after ageing for 100 hours in terms of their physical properties [surface roughness, mass], chemical properties [Fourier Transform Infra-Red (FTIR) spectroscopy], dielectric properties [capacitance and dissipation factor] and electrical properties [voltage breakdown strength and resistance]. The results show that the specimen roughness and mass increase and decrease uniformly, respectively, with increased ageing temperature. Similar degradation results trends with respect to ageing temperature for the dielectric properties and electrical insulation strength is documented. The paper also reports an extended ageing study which investigates early breakdown voltage (EBV) on sample specimens over a much longer time duration, that of up to 1600 hours.**

***Keywords*—Electric machines, ageing, degradation, polymer film, magnet wire, insulation, polyamide-imide (PAI), polyester-imide (PEI), enamel insulated wires, dielectric properties, high voltage breakdown, insulation thermal factors, electric breakdown, partial discharges.**

I. Introduction

Degradation of insulation materials is a major failure mode of electromagnetic coils and electric machines [1], [2]. Insulation materials provide a high resistance medium (typically greater than TΩ/mm) in order to electrically isolate parts in electric machines. A diverse variety of insulation materials are available including polyester-imide (PEI), polyamide-imide (PAI), mica, asphalt, nylon, epoxy resins and meta-aramid calendered papers [3]. These are used in various different ways in electric machines, including: thin-film insulation on magnet wire to prevent strand-to-strand and turn-to-turn short circuits; slot-lining insulation to prevent short circuits between the electromagnetic coils and the frame or lamination stack, and other functions such as electrical isolation of bearings [4], [5], [3].

This work was part of the FUTURE Vehicles Project (EP/I038586/1) funded by the Engineering and Physical Sciences Research Council (EPSRC). D. F. Kavanagh is with the Faculty of Engineering, Institute of Technology Carlow, Ireland. K. N. Gyftakis is with the School of Engineering at the University of Edinburgh. M.D. McCulloch is with the Department of Engineering Science at the University of Oxford, Oxford, OX1 3PJ, UK.

Electrical insulation materials in machines are subjected to a multitude of stresses over the course of their lifetime, including thermal, electrical, ambient (e.g. environmental or chemical) and mechanical factors [6], [7], [8], [9], [4]. Sometimes these are abbreviated as 'TEAM' [3]. These different factors degrade the materials simultaneously and interact with one another, for example, electrical stressing gives rise to temperature increases which in turn gives rise to both chemical and mechanical stressing occurring. Over time insulation materials may become severely degraded to the point where partial discharge occurs, leading to reduced dielectric properties and voltage resistance of the polymeric coatings [10], [11], as well as adhesion problems, delamination, surface erosion, oxidation as well as the formation of treeing and micro-cracks [3], [12]. The occurrence of repetitive partial discharge events greatly accelerates the ageing process further as it then moves from intrinsic ageing into a rapid extrinsic ageing process, which quickly leads to the catastrophic failure of the electric machine as the electromagnetic coils will quickly yield sustained short-circuit conditions [6], [7], [8], [13], [2]. This type of fault mainly occurs in the stator coils, where resulting short circuits can include phase-to-ground, turn-to-turn and phase-to-phase. The latter case occurs to a much lesser extent for concentrated wound machines compared to distributed wound machines.

In the field of condition monitoring of electric machines a large amount of literature exists with respect to stator related faults. Typically, these works are concerned with methods of detection and diagnosis of short-circuits in electric machines [14], [15], [16], [17], [2], [18], [19], [20]. More recently there have been investigations into the fundamental aspects of insulation ageing. In this context, the impact of water ingress on electrically stressed stator coils [9], accelerated ageing on wound model subsections of machines [4], the ageing of calendered insulation paper for for transformers [21] and the impact of fast switching of power electronic converters on insulation health [22], [23] have all been investigated.

Suitable techniques for characterising and modelling insulation in terms of physical, chemical, dielectric and electrical properties are immensely valuable for quality assessment, diagnostics and degradation analysis to determine state of health and also for creating equivalent circuit models [24], [13], [25] for thermal analysis. Related approaches in the literature have investigated ageing on twisted insulation-coated wire pair set-ups [23], [26], motorettes or coils [27], [4] or even full machines [28], [29], [24], [25]. The complexity of such set-ups and the coupled multifaceted ageing phenomena (TEAM) makes the analysis extremely difficult to interpret. To address

this, this experimental study has greatly simplified the sample specimens under test which comprises of sections of rectangular thin-film magnet wire. Rectangular wire was selected as it greatly facilitates the measurement of dielectric properties. These specimens have been exposed to elevated temperatures ranging from 200 C to 275 C. Post ageing the specimens were characterised using physical properties [surface roughness, mass], chemical properties [Fourier Transform Infra-Red (FTIR) spectroscopy], dielectric properties [capacitance, dis-sipation factor and impedance] and electrical properties [voltage breakdown strength and resistance]. This informed the extended ageing study where the focus was on early breakdown voltage V_{EBV} and resistance R_{EBV}. The paper introduces a novel metric β which unifies early breakdown voltage V_{EBV} and resistance R_{EBV}. This metric is valuable as it produces a monotonic behaviour that characterises the severity of the thermal degradation for the thin-film insulation under test.

This paper has been laid out as follows, section II describes some classical background theory on degradation models. The methodology is detailed in section III, which lists the main experimental and characterisation approaches used. Section IV presents an extended ageing study is presented which focuses on the electrical characterisation of aged specimens over 1600 hours. Section V reports the results for the studies described in section III and section IV. The results are discussed and interpreted in section VI. Finally, section VII concludes by summarising the paper and its major findings.

II. Background

Early pioneers of this field, such as Montsinger and Dakin [30], [31], investigated insulation lifetime estimation through a combination of experimental investigation on the materials at the time and the Arrhenius chemical reaction rate theory [32]. Montsinger conducted experiments on oil impregnated paper insulation used in transformers and developed an empirical theory based on the results [30]. Dakin developed a lifetime prediction equation based on the Arrhenius model [31]:

$$\ln \xi = \frac{A}{T} + B \tag{1}$$

where ξ is the lifetime, A and B are constants that depend on the material and T is the absolute temperature. A related rule of thumb often used by designers, known as the 'ten degree' rule, states that beyond the rated temperature the insulation ages twice as fast for every 10 °C rise in temperature [33].

Advances in polymer chemistry have led to sophisticated materials such as PAI, which is used as an insulation coating for copper conductors in electrical machines, which has properties such as high temperature stability and resistance to abrasion and chemical attack. In comparison to other more widely studied materials such as polyimide (PI), less is known about how the properties of materials such as PAI change as they degrade, in particular as they approach the glass transition temperature T_g [34]. Moreover, there has been little investigation into the performance of these materials when coated onto copper conductor magnet wire in composite form [35], [36].

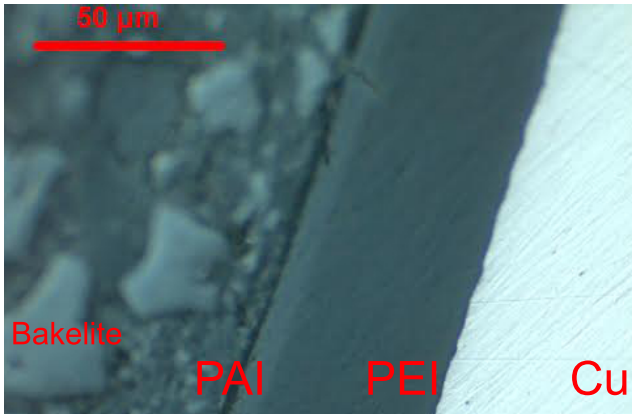

Fig. 1: Microscope image showing a close-up view of the thin-film insulation materials, (PEI and PAI), adhered to the copper substrate material.

Due to the challenge of attributing observed ageing to underlying individual ageing factors in a full machine, coils or motorettes, in this study the experimental approach and analysis was simplified greatly by using specimens of rectangular magnet wire under elevated temperatures in order to investigate thermal degradation phenomena.

III. Methodology

The magnet wire used for these experiments is Class H (IEC 60317-29), which has a basecoat of Polyester-Imide PEI (Terebec MT 533-NM) and an overcoat of Polyamide-Imide PAI (Sivamid 595). The particular wire selected is rectangular wire with dimensions 15.24 mm wide by 2.54 mm thick with an insulation coating thickness of approximately 60 μm, see Fig. 1 and Fig. 2. The thin-film is applied to the copper by drawing the conductor through a bath of PAI solution and then through a die to control the thickness, followed by curing inside an oven.

A. Sample Specimen Preparation

The sample specimens of magnet wire were prepared by cutting the wire into lengths of 350 mm. Care was taken during the preparation to not scratch or damage the surface finish of the insulation coating. The specimen bars were straightened using a clamp and wedge setup to facilitate characterisation measurements. This resulted in 25mm of the ends being bent at an angle of 30°, see Fig. 2 which shows the sample specimens prior to ageing, consisting of six samples as well as Nomex paper, resting on ceramic plates. The ends of the samples were drilled and brass bolt fixtures were inserted to make electrical contact with the copper for the dielectric and breakdown measurements. There were 36 different sample specimens for each of the 7 different temperature *ageing classes* described below, and the results presented are averaged across all 36 samples for each temperature class respectively. The standard error $\sigma_{\bar{x}} = \sigma_x/\sqrt{N}$ is included where σ_x is the standard deviation and N the number of samples in each class.

B. Early-onset Ageing - Study 1

Thermal ageing of the wire samples specimens (class H, 200°C) was achieved by exposing them to the following elevated temperatures continuously in 6 separate temperature controlled fan assisted Lenton thermal chambers: 200 °C, 215 °C, 230 °C, 245 °C, 260 °C, 275 °C. Unaged samples were also used for comparison, giving 7 different *ageing classes* in total. All chambers were sealed and an extraction facility was incorporated to remove any noxious fumes generated during the experiments. The samples were all exposed to the elevated temperature conditions for a duration of 100 h which constitutes the chosen duration of early onset ageing. This period is roughly a quarter of the lifetime at the upper temperature range (275 °C) as defined by the Arrhenius lifetime equation, using the materials data-sheet.

Samples were characterised in terms of their physical, chemical and electrical properties. The physical measurements included surface roughness, mass and visual inspection. The surface roughness was measured using a MicroXAM 3D surface profilometer and optical interferometer. The statistical average roughness parameter used is S_a, as defined in equation 2 below, as defined in [37] and [38].

$$S_a = \frac{1}{MN} \sum_{k=0}^{M-1} \sum_{l=0}^{N-1} |z(x_k, y_l)| \tag{2}$$

where M and N are the numbers of spatial samples in the x and y directions and z is the local roughness height.

For the measurement of mass, the samples were weighed using a precision balance, Adam PW 254, with a precision of 0.1 mg. The chemical measurements consisted of Fourier Transform Infrared (FTIR) Spectroscopy analysis, using a Varian Excalibur FTIR microscope. The absorbance of the insulation material was measured over a wavenumber range of 3500 to 800 cm^{-1}. Above 1500 cm^{-1} the spectra corresponds to the *functional groups* whereas below 1500 cm^{-1} it corresponds to the material *fingerprint* of the polymer.

The parallel plate method [39] was used to make the dielectric measurements. To achieve this a special dielectric measurement probe was created using the ASTM Standard D150 as a reference guide [40], see Fig. 3. The guard electrode removes the effects of stray and fringe capacitance. The dielectric measurements were made using an precision impedance/LCR analyser (PSM1735). One of the measurement leads of the impedance analyser was connected directly to the copper conductor of the rectangular magnet wire specimen and the other lead was connected to the plate electrode of the dielectric measurement probe as shown in see Fig. 3. This probe was placed directly on top of the rectangular wire specimen to measure the dielectric properties. A known mass of 0.5 kg was placed directly on top of the dielectric probe to ensure that a consistent and repeatable pressure was applied to the dielectric material coating on the magnet wire during the measurements. The standard parallel plate capacitance equation as seen in (3) is useful for analysis and interpretation of the results.

$$C = \frac{\epsilon_r \epsilon_0 A}{d} \tag{3}$$

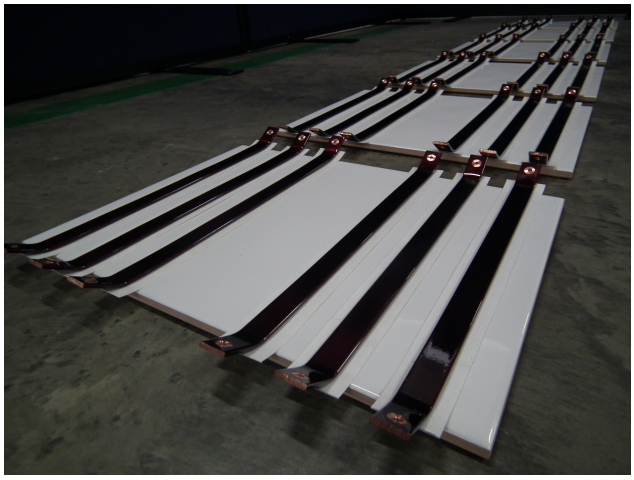

Fig. 2: Showing rectangular magnet wire specimens prior to ageing on a ceramic plates which were then placed inside the six thermal ageing chambers.

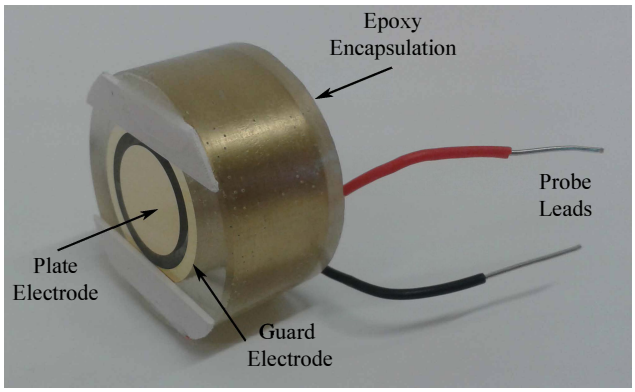

Fig. 3: The dielectric measurement probe used is shown, which was placed directly onto the surface of the rectangular magnet wire specimens to make the measurements using the parallel plate method. The white mounts help to ensure that the plate electrode is correctly placed and aligned.

where C is the capacitance, ϵ_r is the dielectric constant of the thin-film insulation materials (PAI and PEI), ϵ_0 is the permittivity of free space, A is the plate area (A=4.5E-04 m^2 as the radius, r=12 mm) and d is the distance between the plates, which corresponds to the thickness of the insulation coating, in this case $\approx$ 60 μm. The early breakdown voltage was measured using the conductive tape approach as defined in the standard IEC 60851-5 [41]. To make these measurements a Chauvin Arnoux CA6555 15 kV insulation tester was used in DC ramp mode, starting at 1.2 kV and increasing up to the breakdown point. The tester is used in early breakdown mode. In this mode, breakdown is defined as the point when the leakage current reaches 0.1 mA.

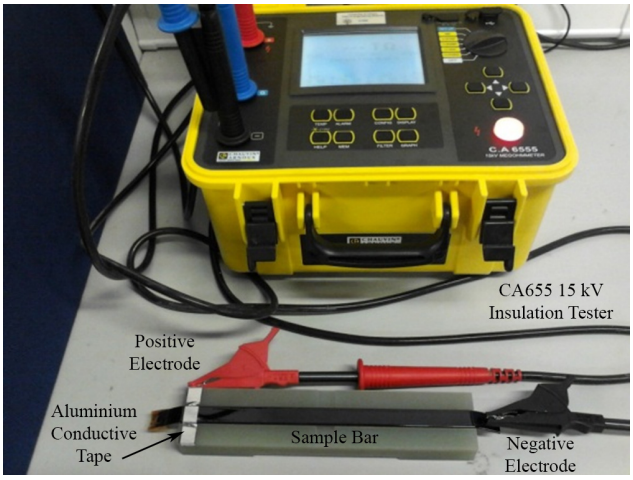

Fig. 4: Early breakdown voltage test set-up.

C. Extended Ageing - Study 2

Groups of 6 sample specimens were thermally stressed at four different temperatures and for different time periods 100h, 200h, 400h, 800h and 1600h. A number of EBV tests has been carried out on different points along each sample. Moreover, 11 healthy and unaged samples were also measured for comparison. The EBV testing is achieved by supplying a voltage ramp from 500 V to 15 kV in a 15 minutes interval. Furthermore, if there is a rapid increase in the current and the current exceeds the critical threshold of 0.2 mA, then the EBV test stops to avoid any damage on the thin-film insulation material. Every insulation point is subjected to three consecutive measurements. This approach was followed after observing that one measurement alone was not enough to indicate the EBV accurately in samples of low degradation levels. A second measurement on the same tested insulation point led to significantly higher EBV, while a third one slightly higher. However more than three repetitions were avoided due to the significantly increased time required for every test and because the accuracy was at acceptable levels. While this particular study focuses on that of electrical breakdown measurements, the reader is also directed towards some of the authors prior literature, [7], [8], [10], [11], where the dielectric measurements of capacitance and dissipation factor have been investigated extensively.

IV. Results

The surface roughness measurements are qualitatively shown in Fig. 5. The unaged sample has a relatively smooth surface with subtle horizontal lines due to the coating process, in the direction of the insulation extrusion. It can be observed that these lines become broader and more pronounced as the ageing exposure temperature increases. The changes in surface roughness is quantified using the a surface roughness parameter S_a. The variation in S_a with respect to temperature is shown in Fig. 6, a trend exists showing the roughness increase from around 6 nm in the unaged sample to about 18 nm at 245 °C ageing and 51 nm at 275 °C ageing.

The results for the measured average masses of the samples at various ageing temperatures are shown in Fig. 7. There is a clear trend of decreasing mass as ageing temperature increases. The mass of copper on the sample specimens was estimated at approximately 101 g with a density of 8.96 g/cm^3 whereas the polymer PAI and PEI layer is only 460 mg with a density of 1.44 g/cm^3.

Fig. 8 shows the FTIR absorbance signatures for the PAI outer insulation layer for the different specimen classes. The spectra are in the range from 2000 to 800 cm^{-1}. Three different regions are highlighted which relate to changes in the molecular structure in the regions of 1596 cm^{-1}, 1258 cm^{-1}, 928 cm^{-1}. These can be referenced to different characteristic molecular bond vibrations. These are annotated on the plot in the regions of interest. The first case suggests increases in the levels of carbon and oxygen double bond stretching. The second case suggests increases in carbon and oxygen single bond stretching with respect to higher exposure temperatures. Finally, the third case suggests that carbon and hydrogen bond vibration peak reduction was replaced by carbon and double carbon bond stretching with respect to the specimens exposed to higher temperatures.

The dielectric impedance measurements are shown in Fig. 9 and Fig. 10, which show the measured capacitance and the dissipation factor (DF) for the different thermal specimen classes. The measurements have been averaged over the frequency range of 100 kHz to 1 MHz. Linear trend lines have been fitted to the measured data to ease the interpretation of the changes which have occurred. A capacitance of 6.2 pF is recorded for the unaged specimens which rises to 8.2 pF for the specimens which were aged at 275 °C as shown in Fig. 9. In the case of dissipation factor, for the unaged specimens a value of 0.03 was measured and at the more elevated temperature class that of 275 °C a value of 0.033 was measured.

The results for insulation resistance R_0 and voltage V_{EBV} tests for the early onset ageing period of 100 h are shown in Fig. 11 and 12, respectively. While the fitted trend line shows a very marginal increase in resistance is recorded across all classes, the measured resistance for the unaged specimen class is 0.7 TΩ compared with to 2 T Ω at the 275 °C which is significant. This increase can be attributed to the oxidation of the copper material at the interface with the polymer film. In Fig. 12 it shown that the high voltage isolation or withstand capability of the insulation is significantly reduced by prolonged exposure to higher temperature ageing even for a relatively short early onset ageing period of 100 h. The unaged case can withstand 8.5 kV before early breakdown occurs, but this dramatically reduces to 5.7 kV for the 275 °C class.

For the extended ageing study as outlined in section IV, measurements were performed on closely inspected insulation. In cases of delamination or any observed damage, measurements were not performed. For example, more than half of the samples were catastrophically damaged under 230 °C after 1600 h. At 245 °C for 1600 h no samples survived. Finally, after 800 h two samples were catastrophically damaged at 200 °C and four at 245 °C. The population size of the tested sample

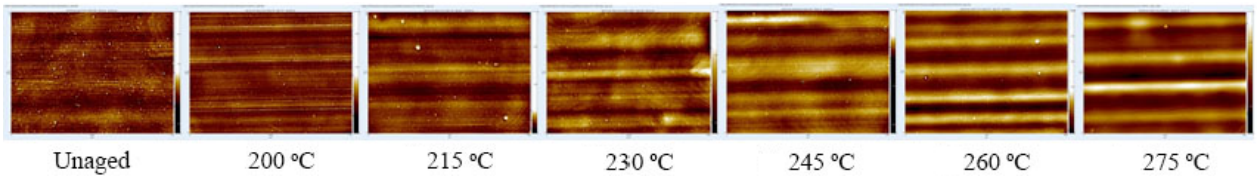

Fig. 5: Measured surface profile at various ageing temperatures for the early onset ageing period of 100 h.

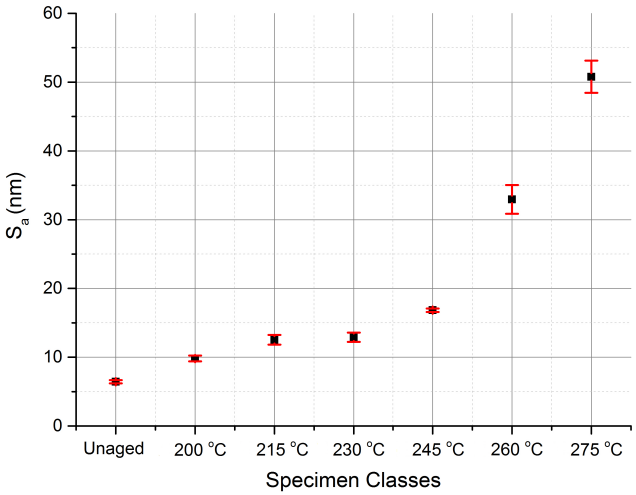

Fig. 6: Average surface roughness S_a of the specimens for the early onset ageing period of 100 h.

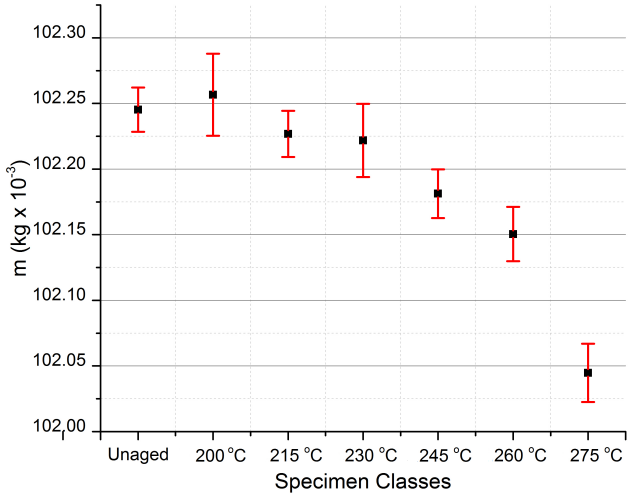

Fig. 7: Average mass of the specimens for the early onset ageing period of 100 h.

points for each degradation group is presented in Table I.

Two pieces of information are extracted from every measurement. The first one concerns the last stored value of insulation thin-film resistance before the breakdown R_0. The

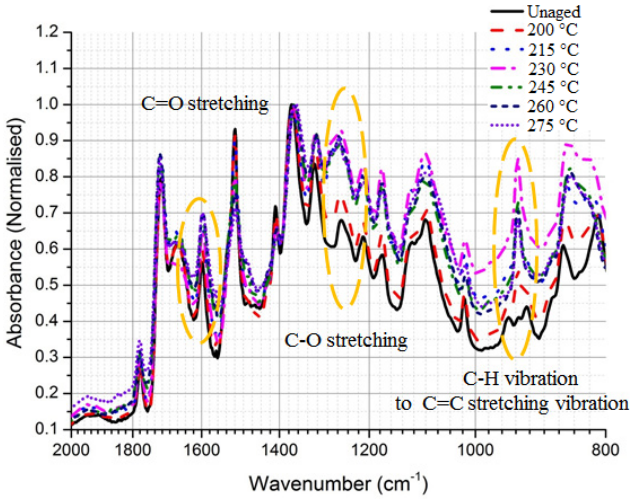

Fig. 8: The FTIR absorbance spectra for the different specimen temperature classes for the early onset ageing period of 100 h.

second one concerns the EBV. The EBV is then divided by the critical threshold current 0.2 mA thus leading to the EBV resistance estimation, R_{EBV}. The analysis of the average insulation thin-film resistance before the breakdown R_0 reveals that although the increase in temperature decreases the overall average resistance, no monotonic behaviour exists in every thermal stress case across the ageing period, see Table II. The EBV value stabilized after the third measurement. For this purpose, the R_{EBV} has been estimated using the last test only. The statistical analysis of the results are shown in Fig. (13 to 16).

In addition, some catastrophic failure modes were observed in the form of meandering cracks typically running the entire length of the magnet wire specimens which show the occurrence of severe delamination. A representative example of this phenomena is shown in Fig. 17.

V. Discussion

The results presented show many material property changes occurring for the different ageing temperatures over a relatively short ageing period. The characteristics of early onset ageing is present which is perhaps best highlighted by the significant reduction in early breakdown voltage capabilities, Fig. 12. However, collectively the results provide a complex set of

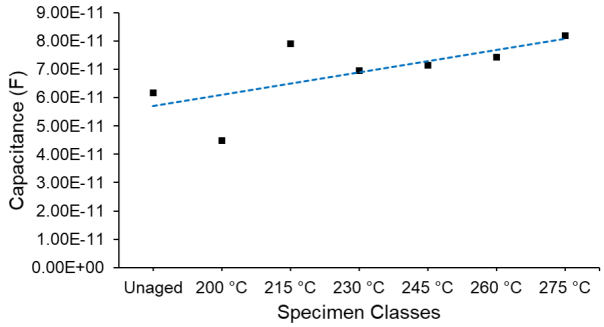

Fig. 9: Capacitance for each of the specimen classes for the early onset ageing period of 100 h.

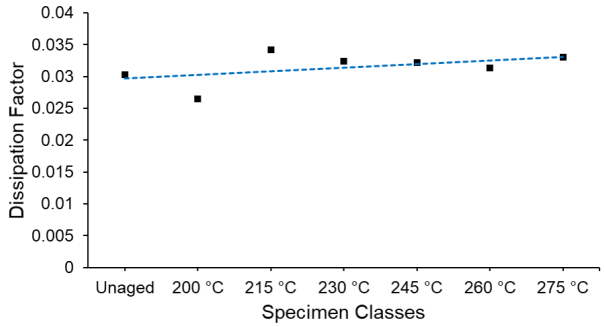

Fig. 10: Dissipation Factor for each of the specimen classes for the early onset ageing period of 100 h.

trends with respect to the different temperature classes and make it difficult to draw conclusive findings.

The physical changes such as surface roughness and mass show correlated trends with respect to increased temperature stressing, with surface roughness increasing and mass decreasing with respect to higher temperature exposure, suggesting physical and perhaps chemical changes. Polymer becomes

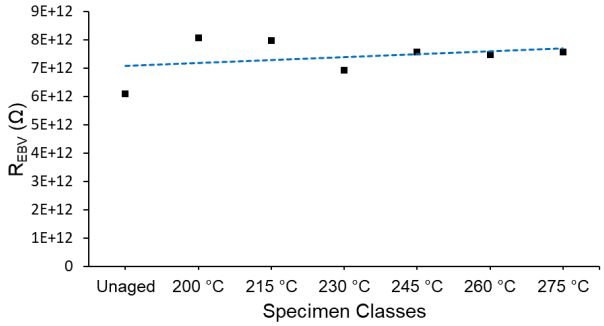

Fig. 11: Resistance R_{EBV} for each of the specimen classes for the early onset ageing period of 100 h.

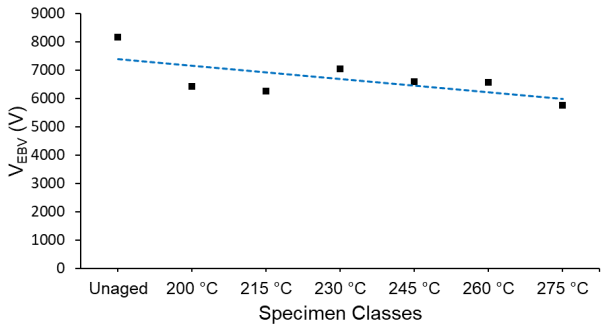

Fig. 12: Early breakdown voltage (V_{EBV}) for each of the specimen classes for the early onset ageing period of 100 h.

TABLE I: THE QUANTITY OF TEST SPECIMEN POINTS

T °C	100 (h)	200 (h)	400 (h)	800 (h)	1600 (h)
200	24	23	23	22	23
215	23	23	24	24	23
230	24	24	22	24	10*
245	24	24	24	16*	0*

*Significantly reduced sample points due to catastrophic failure.

softer towards the glass transition temperature T_g which could lead to changes in surface roughness. The manufacturers (Elantas) list the glass transition for PAI (Sivamid 595) as [42] as 260 °C and 280 °C, with reference to ISO 11357-2 [43].

As magnet wire is a composite material consisting of polymers and copper, there is a significant difference in thermal expansion coefficients of these materials with respect to one another. Copper has a thermal expansion coefficient $\alpha \approx 17 \times 10^{-6}$ K^{-1} but for PAI/ PEI, $\alpha \approx 56 \times 10^{-6}$ K^{-1}. This could lead to the insulation material being mechanically constrained from expanding freely and could be the reason for the roughness 'lines' along the lengths of the specimens as

TABLE II: THE AVERAGE RESISTANCE (GΩ)

T °C	100 (h)	200 (h)	400 (h)	800 (h)	1600 (h)
200[1]	1070	1241	1349	1218	1251
200[2]	1250	1301	1471	1241	1412
200[3]	1188	1354	1536	1348	1433
215[1]	670	1029	1015	1050	996
215[2]	700	1115	1173	1170	1066
215[3]	750	1138	1196	1228	1132
230[1]	685	841	764	830	956
230[2]	669	884	748	849	1031
230[3]	689	881	726	856	983
245[1]	379	327	170	372	CF*
245[2]	360	411	153	310	CF*
245[3]	340	335	153	313	CF*

[1,2,3]Denotes the test iterations and * CF denotes catastrophic failure.

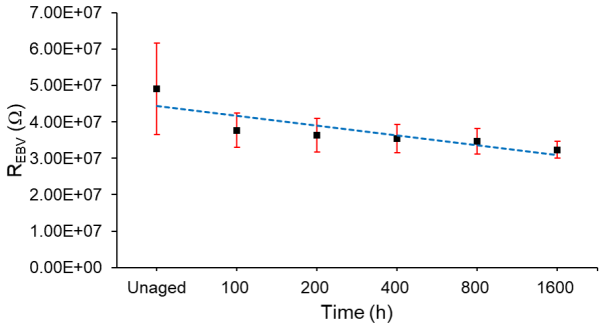

Fig. 13: R_{EBV} Mean±SD for thin-film magnet wire material after exposure to 200 °C for 100 h to 1600 h.

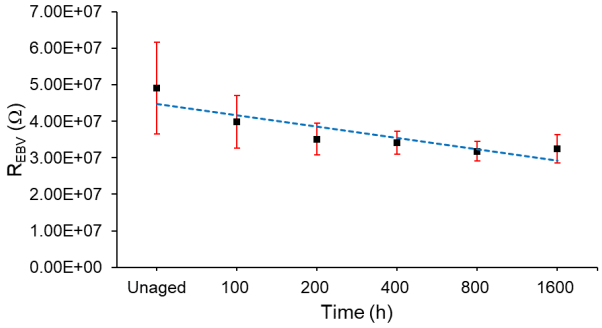

Fig. 14: R_{EBV} Mean±SD for thin-film magnet wire material after exposure to 215 °C for 100 h to 1600 h.

observed in Fig. 5. Other explanations for surface roughness changes could be chemical oxidation of the polymer and possible oxidation and outgassing of the copper underneath the surface. The more elevated temperature specimens are clearly a lot darker in colour, showing qualitative evidence that material chemical ageing processes has occurred at the interface of the polymer coating and the copper substrate material. As

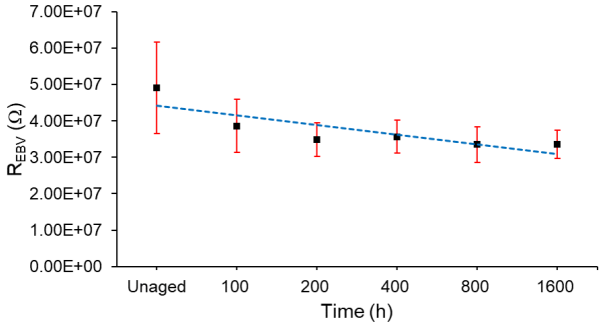

Fig. 15: R_{EBV} Mean±SD for thin-film magnet wire material after exposure to 230 °C for 100 h to 1600 h.

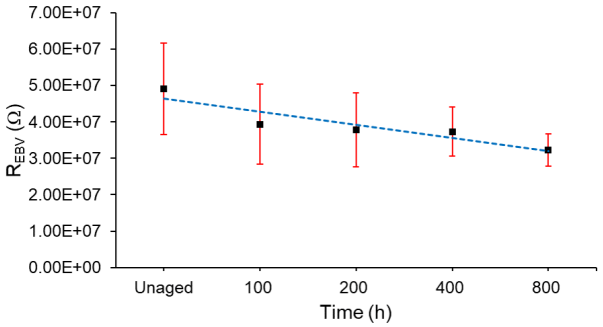

Fig. 16: R_{EBV} Mean±SD for thin-film magnet wire material after exposure to 245 °C for 100 h to 800 h.

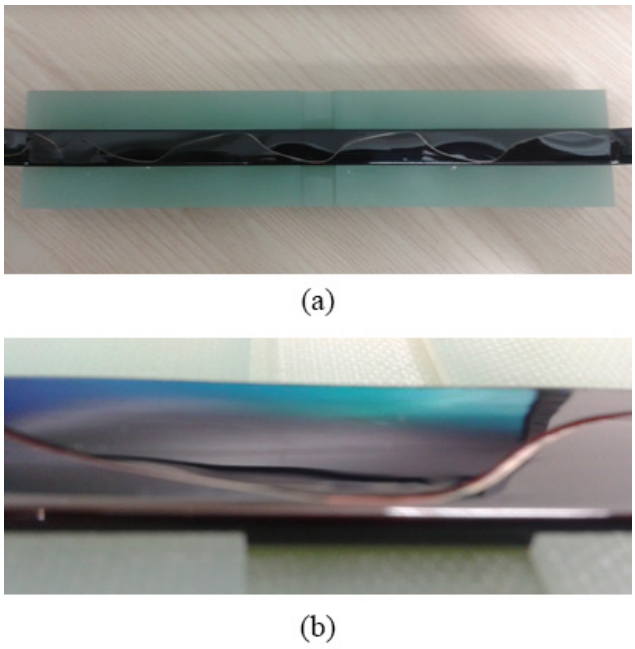

Fig. 17: Catastrophic failure of sample specimen aged at 200 °C (a) crack running the entire length of specimen (b) observed severe delamination underneath the cracked region.

polymers age due to their exposure to high temperatures, their mass reduces due to physical changes caused by evaporation of moisture, solvents, plasticisers, stabilisers and additives. Moreover chemical reactions such as oxidation and breakdown of the molecular bonding structures can result in significant loss of molecular weight [12],[44]. The chemical analysis of the FTIR spectra indicates that during the early stages of ageing, molecular structure changes occur in the polymer material. Three regions in the measured spectra are worth focusing on, these are around the wavenumbers of 1600, 1250 and 950 cm^{-1}, respectively.

These indicate that oxidation of the polymer is occurring at the elevated temperatures since increases in carbon and oxygen

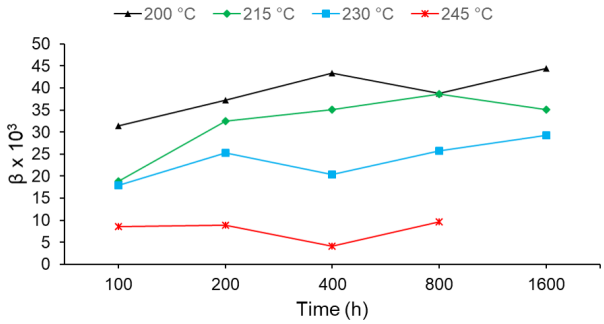

Fig. 18: The relationship of β with respect to the applied thermal stress conditions over time 100 h to 1600 h.

double and single bond vibrations are measured. There are some signs that pyrolysis degradation of the benzene rings is occurring, indicated in the spectra by a loss of carbon and hydrogen single bond vibration which is being replaced with carbon-carbon double bond stretching.

The dielectric measurements recorded show two major trends that of increases in capacitance and increases in dissipation factor with respect to increases in temperature. To help with interpreting this, it is worth referring back to classic capacitance equation (3) and assuming A is constant since the electrode probe plate is not changing, this would suggest that capacitance changes are caused by changes in d and ϵ_r. These heavily relate to the physical property changes that were captured, which shows a significant reduction in the mass of the specimens and an increase in the surface roughness with respect to the higher temperature classes. Also it is important to consider the chemical changes to the polymer material that the FTIR analysis has shown as well as the visual inspection of the specimens post ageing which clearly shows the growth of an oxide layer at the copper-polymer interface. These will significantly impact on the capacitance and the dissipation factor measurements. Hence, drawing conclusions on what is happening to the thin-film coating which gives rise to these dielectric properties changes remains difficult. It does, however, highlight the potential for future investigations into quantifying the changes of three main aspects, measuring that of changes to d, ϵ_r and the oxide layer at the copper polymer interface. The early voltage breakdown studies for 100 h has showed a significant reduction in voltage strength of the materials with respect to their exposure to elevated temperatures.

For the extended ageing study, as described in Section III, for the unaged insulation case a significant number of test measurements were performed on test specimens, 42 in total. For these specimens the mean resistance was recorded as 49.13 MΩ with a standard deviation 12.51 MΩ. This is shown in the plots of Fig. (13) through Fig. (16). For the case of 200 °C, see Fig. (13), a clear trend is present where the mean is shifting downwards and the statistical spread is reducing with respect to increases in the ageing time duration. Similar observations are made for 215 °C, see Fig. (14),. However, for the last measurement at 1600 h, the average seems to be slightly higher than that at 800 h, while the standard deviation increases again. This result is opposing the clear monotonic behaviour of the other studied cases, suggesting a possible critical degradation state has occurred.

The samples aged at 230 °C, see Fig. (15), presents a similar pattern. The average breakdown resistance drops from 100 h to 200 h as expected with a simultaneous reduction of the standard deviation. However, the resistance slightly increases for 400 h and drops again for 800 h. Finally, for 1600 h the average breakdown resistance is slightly higher than that at 800 h while the standard deviation is lower. However, the results for 1600 h are less reliable while some samples of this group were catastrophically damaged during the ageing process. In the last case of 245 °C, see Fig. (16), there is a small drop of the average breakdown resistance from 100 h to 200 h, however the standard deviation does not change. Longer ageing time leads to further reduction of the breakdown resistance while the standard deviation progressively decreases for 400 h and 800 h. The drop of resistance automatically means higher current through the thin-film insulation. To study the dependency of current increase on the applied thermal stress during the breakdown, both resistances before and at early breakdown are required. Simply writing down Ohm's law for before and at the early breakdown occurs, the following two equations can be deduced, (4) and (5), respectively.

$$V_0 = R_0 I_0 \tag{4}$$

Similarly,

$$V_{EBV} = R_{EBV} I_{EBV} \tag{5}$$

As V_0 is the controlled test parameter, and it can be assumed that just before breakdown occurs, $V_0 \approx V_{EBV}$. Hence, an expression for the normalised increase in current, denoted here as β, is defined in equation (6).

$$\beta = \frac{\Delta I}{I_0} = \frac{I_{EBV} - I_0}{I_0} = \frac{R_0 - R_{EBV}}{R_{EBV}} \tag{6}$$

The parameter β was calculated for all of the test cases and the results are summarized in Fig.18. The results show that as the temperature of aging increases then the leakage current at breakdown I_{EBV} and the resistance R_{EBV} at breakdown reduces. Accordingly, this reduction leads to an increase in the metric β across time as the magnet wire degrades. This monotonic ageing trend has been observed for the four different ageing temperature profiles which were part of this research study.

This paper has presented different measurement results and trends for physical, chemical, dielectric and electrical measurements, which offers a collective analysis approach to help interpret the result findings. The degradation phenomena and behaviour of polymer film used on magnet wire under thermal ageing conditions is complex and multifaceted. In real-world electric machines the thermal ageing process is more complex as thermal gradients and hot-spots are present within the electromagnetic coils.

VI. Conclusion

This paper has focused on characterising the thermal degradation phenomena of polymer film insulation (PAI/PEI) on magnet wire for electromagnetic coils. Two studies have be reported, the first being an *early onset ageing* study (100 h) which explored, physical, chemical, dielectric and electric properties and the second being an *extended ageing* study (1600 h), which focused solely on electric properties. This work has clearly shown that the ageing phenomena and characterisation of thin-film magnet wire is highly complex and one that requires careful treatment and examination. Electric machine designers and equipment manufacturers should appreciate the limitations of the widely used Arrhenius lifetime law and the 'ten degree' rule. While these approaches have theoretical and experimental foundations, the results and associated phenomena strongly suggest that the ageing behaviours and degradation mechanisms of polymer film on magnet wire is significantly more complex. Moreover, advancements in polymer chemistry and manufacturing processes has changed substantially since the early lifetime phenomena studies on insulation materials was undertaken in the 1930's and 1940's, and therefore there is a need to carefully re-examine the suitability of these for magnet wire which is a complex composite material. The paper has also introduced a new metric β, which unifies two related parameters, that of I_{EBV} and R_{EBV} for high voltage electric breakdown characterisation and testing. This metric produces a monotonic trend which increases over the ageing period, and hence offers a valuable way to characterise the severity of the insulation degradation.

References

[1] D. F. Kavanagh, K. N. Gyftakis, and M. D. McCulloch, "Early-onset degradation of thin-film magnet wire insulation for electromechanical energy converters," *Proceedings of the 2019 IEEE 12th International Symposium on Diagnostics for Electrical Machines, Power Electronics and Drives (SDEMPED)*, 2019.

[2] S. Grubic, J. M. Aller, B. Lu, and T. G. Habetler, "A survey on testing and monitoring methods for stator insulation systems of low-voltage induction machines focusing on turn insulation problems," *IEEE Transactions on Industrial Electronics*, vol. 55, no. 12, pp. 4127–4136, 2008.

[3] G. C. Stone, E. A. Boulter, I. Culbert, and H. Dhirani, *Electrical Insulation for Rotating Machines - Design, Evaluation, Aging, Testing and Repair*. IEEE Press Series on Power Engineering, 2004.

[4] M. Farahani, E. Gockenbach, H. Borsi, K. Schäfer, and M. Kaufhold, "Behavior of machine insulation systems subjected to accelerated thermal aging test," *IEEE Transactions on Dielectrics and Electrical Insulation*, vol. 17, no. 5, pp. 1364–1372, 2010.

[5] A. Muetze and A. Binder, "Don't lose your bearings," *IEEE Industry Applications Magazine*, vol. 12, no. 4, pp. 22–31, 2006.

[6] L. L. Korcak and D. F. Kavanagh, "Thermal accelerated aging methods for magnet wire: A review," *Proceedings of the 2018 International Conference on Diagnostics in Electrical Engineering (Diagnostika)*, 2018.

[7] K. N. Gyftakis, M. Sumislawska, D. F. Kavanagh, D. A. Howey, and M. D. McCulloch, "Dielectric characteristics of electric vehicle traction motor winding insulation under thermal aging," *IEEE Trans. Ind Appl.*, vol. 52, no. 2, pp. 1398–1404, 2016.

[8] M. Sumislawska, K. N. Gyftakis, D. F. Kavanagh, M. D. McCulloch, K. J. Burnham, and D. A. Howey, "The impact of thermal degradation on properties of electrical machine winding insulation material," *IEEE Trans. Ind Appl.*, vol. 52, no. 4, pp. 2951–2960, 2016.

[9] M. A. R. M. Fernando, W. M. L. B. Naranpanawa, and R. M. H. M. Rathnayake, "Condition assessment of stator insulation during drying, wetting and electrical ageing," *IEEE Transactions on Dielectrics and Electrical Insulation*, vol. 20, no. 6, pp. 2081–2090, 2013.

[10] M. Sumislawska, K. N. Gyftakis, D. F. Kavanagh, M. D. McCulloch, K. J. Burnham, and D. A. Howey, "The impact of thermal degradation on electrical machine winding insulation," *Proceedings of the 2015 IEEE 10th International Symposium on Diagnostics for Electrical Machines, Power Electronics and Drives (SDEMPED)*, 2015.

[11] K. N. Gyftakis, M. Sumislawska, D. F. Kavanagh, D. A. Howey, and M. D. McCulloch, "Dielectric characteristics of electric vehicle traction motor winding insulation under thermal ageing," *Proceedings of the 2015 IEEE 15th International Conference on Environment and Electrical Engineering (EEEIC)*, 2015.

[12] L. A. Dissado and J. C. Fothergill, *Electrical Degradation and Breakdown in Polymers*. IEE Materials and Devices Series 9, Peter Peregrinus Ltd, 1992.

[13] D. F. Kavanagh, D. A. Howey, and M. D. McCulloch, "An applied laboratory characterisation approach for electric machine insulation," *Proceedings of the 2013 9th IEEE International Symposium on Diagnostics for Electric Machines, Power Electronics and Drives (SDEMPED)*, 2013.

[14] D. Díaz, M. C. Amaya, and A. Paz, "Inter-turn short-circuit analysis in an induction machine by finite elements method and field tests," *Proceedings of the XXth International Conference Electrical Machines (ICEM)*, pp. 1757–1763, 2012.

[15] L. Frosini, E. Bassi, and L. Girometta, "Detection of stator short circuits in inverter-fed induction motors," *Proceedings of the 38th Annual Conference on IEEE Industrial Electronics Society*, pp. 5102–5107, 2012.

[16] K. Kim, "Simple online fault detecting scheme for short-circuited turn in a pmsm through current harmonic monitoring," *IEEE Transactions on Industrial Electronics*, vol. 58, no. 6, pp. 2565–2568, 2011.

[17] J. Urresty, J. Riba, H. Saavedra, and L. Romeral, "Detection of inter-turns short circuits in permanent magnet synchronous motors operating under transient conditions by means of the zero sequence voltage," *Proceedings of the 14th European Conference on Power Electronics and Applications*, pp. 1–9, 2011.

[18] P. Tavner, "Review of condition monitoring of rotating electrical machines," *IET Power Electric Applications*, vol. 2, no. 4, pp. 215–247, 2008.

[19] M. A. Awadallah, M. M. Morcos, S. Gopalakrishnan, and T. W. Nehl, "Detection of stator short circuits in vsi-fed brushless dc motors using wavelet transform," *IEEE Transactions on Energy Conversion*, vol. 21, no. 1, pp. 1–8, 2006.

[20] S. M. A. Cruz and A. J. M. Cardoso, "Diagnosis of stator inter-turn short circuits in dtc induction motor drives," *IEEE Transactions on Industry Applications*, vol. 40, no. 5, pp. 1349–1360, 2004.

[21] M. Wen, J. Song, Y. Song, Y. Liu, C. Li, and P. Wang, *IEEE Transactions on Dielectrics and Electrical Insulation*, vol. 20, no. 6, pp. 1998–2008, 2013.

[22] A. Cavallini, D. Fabiani, and G. C. Montanari, "Power electronics and electrical insulation systems - part 1: Phenomenology overview," *IEEE Electrical Insulation Magazine*, vol. 26, no. 3, pp. 7–15, 2010.

[23] F. Guastavino, A. Ratto, E. Torello, and G. Biondi, "Aging tests on nanostructured enamels for winding wire insulation," *IEEE Transactions on Industrial Electronics*, vol. 61, no. 10, pp. 5550–5557, 2014.

[24] M. Sumislawska, O. Agbaje, D. F. Kavanagh, and K. J. Burnham, "Equivalent circuit model estimation of induction machines under elevated temperature conditions," *Proceedings of the 2014 UKACC International Conference on Control (CONTROL)*, 2014.

[25] O. Agbaje, D. F. Kavanagh, M. Sumislawska, D. A. Howey, M. D. McCulloch, and K. J. Burnham, "Estimation of temperature dependent equivalent circuit parameters for traction-based electric machines," *Proceedings of the IET Hybrid and Electric Vehicles Conference 2013 (HEVC 2013)*, 2013.

[26] H. Nakaya, M. Kozako, M. Hikita, M. Ohya, D. Muto, and K. Tomizawa, "Partial discharge inception voltage of enamel twisted-pair samples with several laminated insulation layers," *Annual Report Conference on Electrical Insulation and Dielectric Phenomena*, pp. 1270–1273, 2013.

[27] C. Rusu-Zagar, P. Notingher, V. Navrapescu, G. Mares, G. Rusu-Zagar, T. Setnescu, and R. Setnescu, "Method for estimating the lifetime of electric motors insulation," *8th International Symposium on Advanced Topics in Electrical Engineering (ATEE)*, pp. 1–6, 2013.

[28] T. G. Arora, M. V. Aware, and D. R. Tutakne, "Accelerated insulation aging in phase angle controlled single phase induction motors," *IEEE Region 10 Conference TENCON*, 2009.

[29] D. Fabiani, A. Cavallini, and G. Montanari, "Aging investigation of motor winding insulation subjected to pwm-supply through pd measurements," *Annual Report Conference on Electrical Insulation and Dielectric Phenomena*, pp. 434–437, 2005.

[30] V. Montsinger, "Loading transformers by temperature," *Transactions of the American Institute of Electrical Engineers AIEE*, vol. 49, pp. 776–790, 1930.

[31] T. Dakin, "Electrical insulation deterioration treated as a chemical rate phenomenon," *Transactions of the American Institute of Electrical Engineers AIEE*, vol. 67, pp. 113–122, 1948.

[32] F. Kielmann and M. Kaufhold, "Evaluation analysis of thermal ageing in insulation systems of electrical machines - a historical review -," *IEEE Transactions on Dielectrics and Electrical Insulation*, vol. 17, no. 5, pp. 1373–1377, 2010.

[33] B. R. Sathyanarayana, G. T. Heydt, and M. L. Dyer, "Distribution transformer life assessment with ambient temperature rise projections," *Electric Power Components and Systems*, vol. 37, no. 9, pp. 1005–1013, 2009.

[34] S. Diaham, M. L. Locatelli, T. Lebey, and S. Dinculescu, "Dielectric and thermal properties of polyamid-imide (pai) films," *Annual Report Conference on Electrical Insulation and Dielectric Phenomena*, pp. 482–485, 2009.

[35] B. Petitgas, G. Seytre, O. Gain, G. Boiteux, I. Royaud, A. Serghei, A. Gimenez, and A. Anton, "High temperature aging of enameled copper wire-relationships between chemical structure and electrical behaviour," *Annual Report Conference on Electrical Insulation and Dielectric Phenomena*, 2011.

[36] F. Aymonino, T. Lebey, D. Malec, C. Petit, J. S. Michel, A. Anton, and A. Gimenez, "Degradation and dielectrics measurements of rotating machines insulation at high temperatures (200-400°c)," *IEEE Annual report on ICSD Conference*, pp. 130–133, 2007.

[37] ISO, *25178-2:2012 Geometrical product specifications (GPS) — Surface texture: Areal — Part 2: Terms, definitions and surface texture parameters*, 2012.

[38] ASME, *B46.1 - 2009 Surface Texture (Surface Roughness, Waviness, and Lay)*, 2009.

[39] T. T. Grove, M. F. Masters, and R. E. Miers, "Determining dielectric constants using a parallel plate capacitor," *American Journal of Physics*, vol. 73, no. 1, pp. 52–56, 2005.

[40] ASTM, *D150-18, Standard Test Methods for AC Loss Characteristics and Permittivity (Dielectric Constant) of Solid Electrical Insulation*, 2018.

[41] IEC, *60851-5:2008+AMD1:2011+AMD2:2019 Winding wires - Test methods - Part 5: Electrical properties*, 2019.

[42] Elantas, "Sivamid 595 rev 1 polyamide-imide magnet wire enamel," *Technical Data Sheet*, 2016.

[43] ISO, *11357-2:2013(en) Plastics — Differential scanning calorimetry (DSC) — Part 2: Determination of glass transition temperature and glass transition step height*, 2013.

[44] G. M. Swallowe, *Mechanical Properties and Testing of Polymers*. Kluwer Academic Publishers, 1999.

Darren F. Kavanagh (M'09) received the Ph.D. degree in acoustic signal processing from Trinity College Dublin, Dublin, Ireland, in 2011. Darren is a Lecturer, Principal Investigator and Programme Director for BEng Electronic Engineering with the Institute of Technology Carlow. Prior to this, he was a Postdoctoral Researcher with the University of Oxford, Oxford, U.K. He has gained valuable academic experience at educational institutions such as the University of Oxford; Trinity College Dublin; and at Technological University Dublin. He has also benefited greatly from industrial experience at Alcatel Lucent-Bell Laboratories, Intel, and Xilinx. He has projects funded by EI; IRC; SFI, SEAI, Campus France and various collaborative industry partners. Currently, he is interested in the broad topic of applied embedded systems for industrial applications and developing industrial-academic partnership opportunities.

Konstantinos N. Gyftakis (M'11, SM'20) was born in Patras, Greece, in May 1984. He received the Diploma in Electrical and Computer Engineering from the University of Patras, Patras, Greece in 2010. He pursued a Ph.D in the same institution in the area of electrical machines condition monitoring and fault diagnosis (2010-2014). Furthermore, he worked as a Post-Doctoral Research Assistant in the Dept. of Engineering Science, University of Oxford, UK (2014-2015). Then he worked as Lecturer (2015-2018) and Senior Lecturer (2018-2019) in the School of Computing, Electronics and Mathematics and as an Associate with the Research Institute for Future Transport and Cities, Coventry University, UK. Since 2019, he has been a Lecturer in Electrical Machines and a Member of the Institute for Energy Systems, University of Edinburgh, UK. His research interests focus on fault diagnosis, condition monitoring and degradation of electrical machines. He has authored/co-authored more than 100 papers in international scientific journals and conferences and a chapter for the book: "Diagnosis and Fault Tolerance of Electrical Machines, Power Electronics and Drives", IET, 2018. He is an IEEE Senior Member, as well as member of the IEEE IAS and IEEE IES.

Malcolm D. McCulloch (S'88–M'89) received the B.Sc. (Eng.) and Ph.D. degrees in electrical engineering from the University of the Witwatersrand, Johannesburg, South Africa, in 1986 and 1990, respectively. In 1993, he joined the University of Oxford, Oxford, U.K., to head up the Energy and Power Group, where he is currently an Associate Professor with the Department of Engineering Science. He is active in the areas of electrical machines, transport, and smart grids. His work addresses transforming existing power networks, designing new power networks for the developing world, developing new technology for electric vehicles, and developing approaches to integrated mobility.